
Display motion blur: Comparison of measurement methods

Andrew B. Watson (SID Senior Member)

Abstract — Motion blur is a significant display property for which accurate, valid, and robust measurement methods are needed. Recent motion-blur measurements of a set of eight displays by a set of six measurement devices provided an opportunity to evaluate techniques of measurement and analysis. Both the raw data waveforms collected by each device and the metrics derived from those waveforms were examined. Significant discrepancies between instruments and variability within instruments were found. A new motion-blur metric (GET) that exhibits increased robustness and reduced variability relative to existing metrics is proposed.

Keywords — MPRT, BET, EBET, PBET, GET.

DOI # 10.1889/SID18.2.179

1 Objective and background

Many modern display technologies, notably LCD, are subject to motion blur.¹ Motion blur arises when the eye tracks a moving image, while the display presents individual frames that persist for significant fractions of a frame duration, or longer. As a result, the image is smeared across the retina during the frame duration.

There have been a number of attempts to characterize motion blur in a systematic and meaningful way. Most of these involve estimating the width of an edge subjected to motion blur. This edge can be captured in any of three ways.^{2,3} The first method employs a pursuit camera (PC) that tracks a vertical edge (between two gray levels) as it moves horizontally across the screen.⁴ The camera is simulating the eye as it pursues the moving edge. The result, after averaging over time, is a picture of the blurred edge. After averaging over the vertical dimension (orthogonal to the motion), a one-dimensional waveform representing the cross-section of the blurred edge can be obtained. It describes relative luminance (a linear function of luminance) as a function of horizontal position in pixels. We will call this the moving edge spatial profile (MESP). When recorded at several speeds of edge motion, the waveforms are usually found to correspond when the horizontal scale is divided by the speed. Therefore, it is conventional to rescale the horizontal axis of the profile (pixels) by dividing by the speed (pixels/frame) to obtain a waveform that is a function of time (frames). We call this the moving edge temporal profile (METP). It is also conventional to characterize the width of the METP in terms of the time interval between 10% and 90% points of the curve. This quantity is called the blur edge time (BET) and is reported in milliseconds.

The second method employs a stationary high-speed camera. With a sufficiently high frame rate, it is possible to

capture a sequence of frames, that, with appropriate shifting and adding, can also yield a record of the MESP and thereby the METP. The high-speed camera avoids the mechanical challenges of the pursuit camera. We call this method digital pursuit (DP).

The third method employs a fixed non-imaging detector such as a photodiode, which measures the luminance over time as the display is switched from one gray level to another. This temporal step response is then convolved with a pulse of duration equal to the hold time (for an LCD, typically one frame), to obtain another version of the METP.⁵⁻⁸ We call this the temporal step (TS) method. This last method relies on an assumption that all pixels are independent. It has been demonstrated to be accurate in many cases,^{2,3} but may fail when motion-dependent processing is present.

Outstanding questions remain regarding the accuracy and agreement among these various methods, and also regarding the analysis of the METP. In February 2008, a unique opportunity was provided to address some of these questions. Under the auspices of the International Committee on Display Metrology,⁹ an experiment was conducted in which eight flat-panel displays were measured by six different motion-blur measuring instruments. The testing facility was provided by Samsung, Inc., in Seoul, Korea. The objective of this report is to discuss preliminary results from that experiment. The primary focus will be on the degree of agreement among methods and on the analysis of the METP.

Several previous reports have compared measurement methods on several displays,^{2,3,10} but have not had access to the large number of displays and measurement devices assessed here. A preliminary version of this report was presented at the 2009 SID Symposium.¹¹

Expanded revised version of a paper presented at the 2009 SID International Symposium (Display Week 2009) held May 31–June 5, 2009 in San Antonio, Texas, U.S.A.

The author is with the NASA Ames Research Center, MS 262-2, Moffett Field, CA 94035; telephone 650/604-5419, e-mail: andrew.b.watson@nasa.gov.

This is a contribution of the NASA Ames Research Center and is not subject to copyright.

TABLE 1 — Displays under test.

DUTID	Type	Size	Resolution	Features
001	LCD	21	1280x768	BLI
002	LCD	46	1920x1080	HCFL, SBL, 120 Hz
003	LCD	52	1920x1080	120 Hz
004	LCD	24	1920x1200	
005	LCD	32	1920x1080	OD
006	PDP	65	1920x1080	OD
007	LCD	65	1920x1080	
008	LCD	42	1366x768	HCFL, SBL

BLI is the Black-level insertion; HCFL is the hot-cathode fluorescent lamp; SBL is the scanning backlight; OD is the overdrive.

2 Methods

2.1 Displays

Each display [device under test (DUT)] was identified by a three-digit code (DUTID) to preserve anonymity of the display manufacturers. The various displays are identified in Table 1. The set of displays included both LCDs and PDPs, and a range of technologies to combat motion blur (black-level insertion, hot-cathode fluorescent lamp, scanning backlight, overdrive, 120-Hz frame rate).^{12,13}

2.2 Measurement devices

The six light-measurement devices (LMD) are described in Table 2. Each is identified by a code (LMDID) in order to preserve anonymity of the proponents.

2.3 Procedures

The eight displays were assembled in one large room. Each team associated with one LMD collected measurements with their device from as many displays as possible over the course of 2 days. Room illumination was dim but not precisely controlled.

The experimental conditions consisted of 20 gray–gray transitions, consisting of the pairwise combinations of gray levels 0, 91, 139, 150, and 255. Two speeds of edge motion were used: 8 and 16 pixels/frame. The basic data requested of each team were (1) estimates of BET and (2) METP or MESP waveforms for each of the 40 conditions.

TABLE 2 — Motion-blur measurement devices.

LMDID	Method	Method ID
120560	Digital pursuit	DP
222498	Time step response	TS
240456	Digital pursuit	DP
505301	Digital pursuit	DP
616000	Pursuit camera	PC
979225	Pursuit camera	PC

Following the experiment, data were submitted electronically to the author for analysis. A standard template was provided for data submission, but in no instance did the data exactly follow the template, so subsequent editing of the data files was required. Transcription of data by the proponents, and editing by the author, introduce possible sources of error.

2.4 Waveform standardization

Before further analysis, all submitted waveforms were converted to a standard form. Some were submitted as temporal step responses, which were converted to METP by convolution with a pulse of duration of one frame. Some waveforms were submitted as a blurred pulse rather than a blurred edge. These were split into leading and trailing blurred edges. Where necessary, the spatial coordinates of MESP were converted from camera pixels to display pixels. Finally, all MESP were converted to METP, by dividing the horizontal coordinate (pixels) by the edge speed (pixels/frame).

3 Results

A total of 36 data sets were obtained, each consisting of a particular LMD applied to a particular DUT. Altogether, these comprised 1360 METP, and 1281 BET estimates (some teams submitted waveforms but not BET data for certain conditions). An example of one METP is shown in Fig. 1. This particular METP exhibits considerable noise. This is largely because this is a small transition between nearby gray levels {139, 150}. Note that the curve is expressed (like all METP) as a function of time in frames.

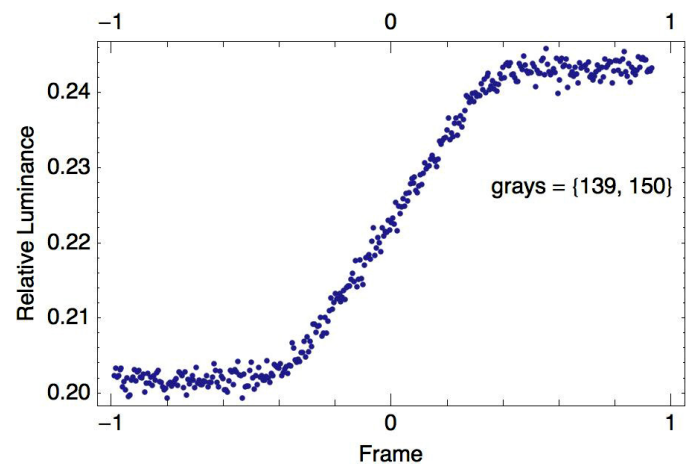


FIGURE 1 — Example of METP. Details: LMDID = 616000, DUTID = 001, gray levels = {139,150}, speed = 16 pixels/frame.

3.1 GET metric

To provide a summary description of each curve, we have fit it with a cumulative Gaussian of the form

$$G(t) = B + (E - B) \int_{-\infty}^t \frac{1}{\sqrt{2\pi}\sigma} \exp\left(-\frac{(x-\mu)^2}{2\sigma^2}\right) dx \quad (1)$$

$$= E + \frac{B-E}{2} \operatorname{erfc}\left(\frac{x-\mu}{\sqrt{2}\sigma}\right),$$

where B and E are beginning and ending relative luminance values, t is time in frames, μ is the mean and σ is the standard deviation of the Gaussian, and erfc is the complementary error function. The parameter σ , in frames, is a useful estimate of the width of the Gaussian. It can easily be converted to an estimate of BET. We call this estimate Gaussian Edge Time (GET) given by

$$\text{GET} = 2563\sigma/w, \quad (2)$$

where w is the frame rate in Hz. The constant 2563 includes factors to convert from milliseconds to seconds, and from standard deviation to a 10–90% width.

By default, for additional accuracy, the fitting was done twice. First, the mean and standard deviation were estimated from the complete waveform. Then the waveform was trimmed to the mean plus and minus four standard deviations, and the fitting was repeated. This avoids distortions due to deviations far from the actual edge.

As noted in the appendix, we provide a supplementary file illustrating the fit to each of the 1360 METP.

3.2 Fit of the Gaussian

To quantify the fit of the Gaussian to the waveforms, we have first created a filtered version of each METP. This was obtained by filtering the waveform with a Gaussian kernel with a standard deviation of 0.025 frames. The purpose of this was to remove the noise from the sampled empirical waveform. The choice of standard deviation reflects a compromise between noise removal and signal preservation. To remove noise, we want a value as large as possible, but we found that values above 0.025 frames significantly attenuated signal components, such as ripples in the waveforms for DUTID 006 (PDP) (see Fig. 2 for examples). We then computed the RMS error between the fitted Gaussian and the smoothed waveform. The error was computed only over the trimmed waveform (mean plus and minus four standard deviations). This quantity was then normalized by the total amplitude for the waveform [by the absolute value of the difference between E and B in Eq. (1)]. This yields a measure of the departure between the two waveforms that is independent of the total amplitude or the sample frequency or the edge width. For visual reference, we show two examples in Fig. 2 of the original sampled waveform, the smoothed version, and the fitted Gaussian, along with the

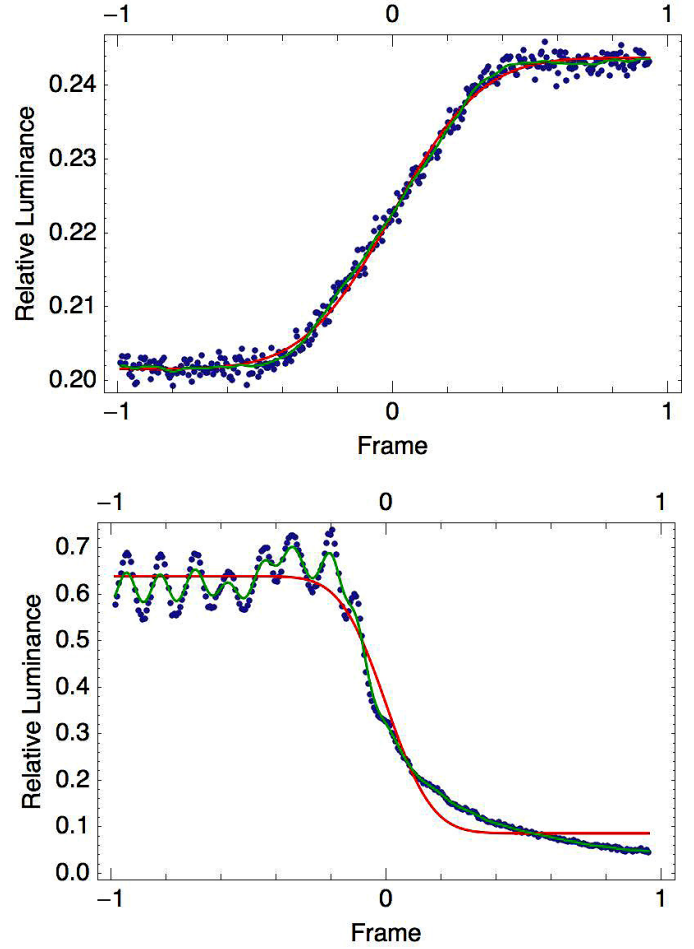


FIGURE 2 — Examples of the fit of a Gaussian (red curve) to the METP (blue points), with smoothed waveform (green curve) also shown. The estimate of sigma is shown. (a) This is the same METP shown in Fig. 1, (b) LMDID = 616000, DUTID = 006.

estimated value of sigma. For these examples, the computed normalized RMS error is 0.016 and 0.061.

The Gaussian provided a reasonable fit to nearly all of 1360 METP. This is quantified in Fig. 3, where we show the distribution of errors for all collected waveforms, and in Fig. 4, in which individual distributions are shown for each

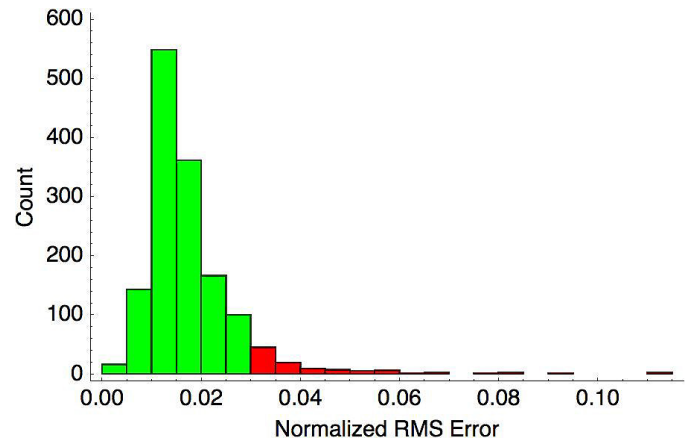


FIGURE 3 — Distribution of normalized RMS errors fits a Gaussian to the METP for all cases. Errors greater than 0.03 are colored red. These comprise about 7% of the total.

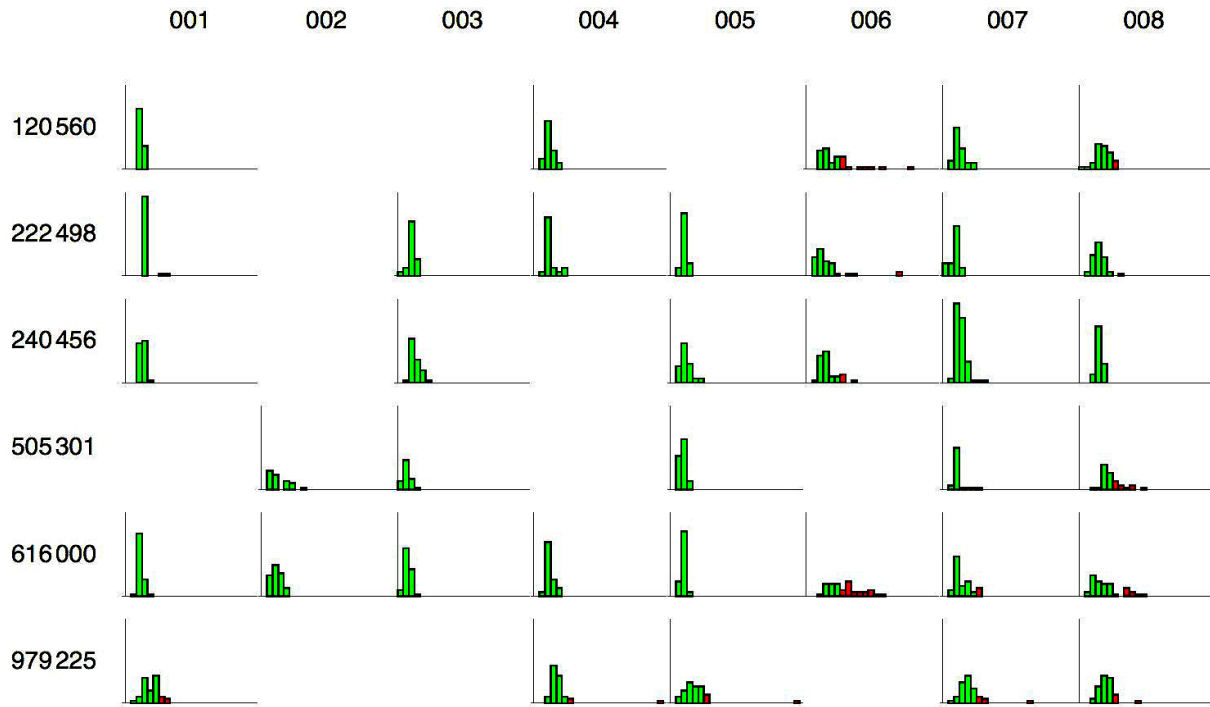


FIGURE 4 — Distributions of Gaussian fit error for each of the 36 pairings of LMDID (shown at the left) and DUTID (shown at the top). Values greater than 0.03 are colored red. The horizontal scale of each panel is the same as in Fig. 3; the vertical range is {0,40}.

LMDID and DUTID. As can be seen, most (about 93%) of the cases have an error less than 0.03.

The cases in which the Gaussian provides a poor fit are almost always cases in which the METP exhibits large non-monotonicities (undershoot, overshoot, ringing), and these occur primarily with the PDP (DUTID = 006) and the strobing backlight (DUTID = 008). It is worth noting that for these cases, conventional measures such as BET function poorly as well. Other poor fits occur at the smallest gray-level transition {139–150} which for some LMD yielded very noisy and poorly defined METP.

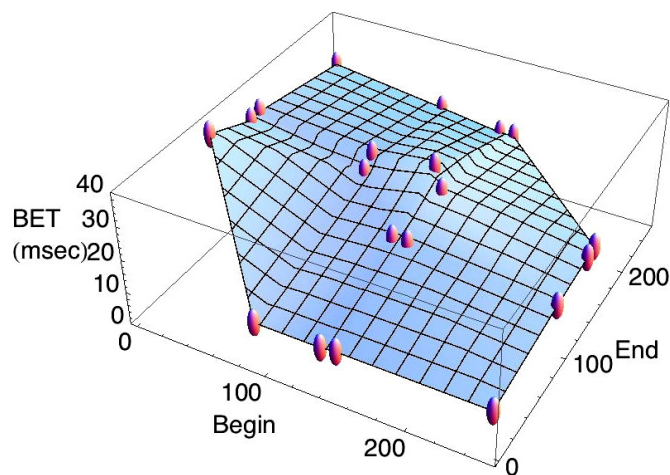


FIGURE 5 — BET data for 8 pixel/frame for LMDID 120560 and DUTID 004.

3.3 BET results

We collected a total of 1281 BET estimates from the measurement teams. These were derived by each team through proprietary analyses of their own instrument data. An example of one set is shown in Fig. 5. It shows BET as a function of the beginning and ending gray levels of the edge. In this particular case, there is considerable variation in BET with gray level.

To provide a summary picture of these results, we have computed the mean and standard deviation, over both gray-level pair and edge speed, for each combination of LMD and DUT. It must be borne in mind that this measure mixes

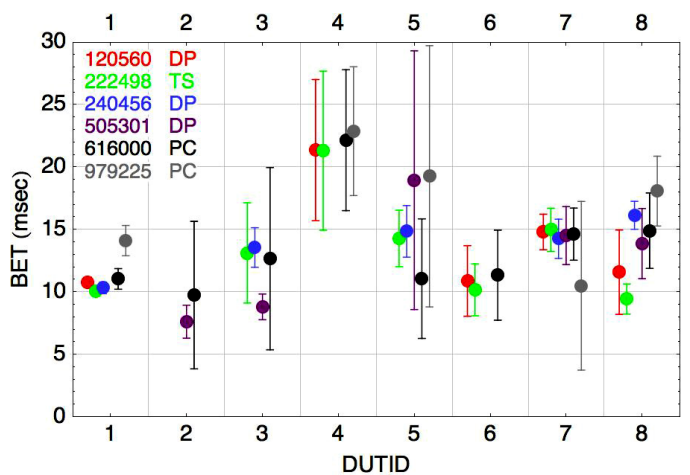


FIGURE 6 — Mean and standard deviation of BET estimates for eight DUT and six LMD. In the key each LMDID is accompanied by the LMD method.

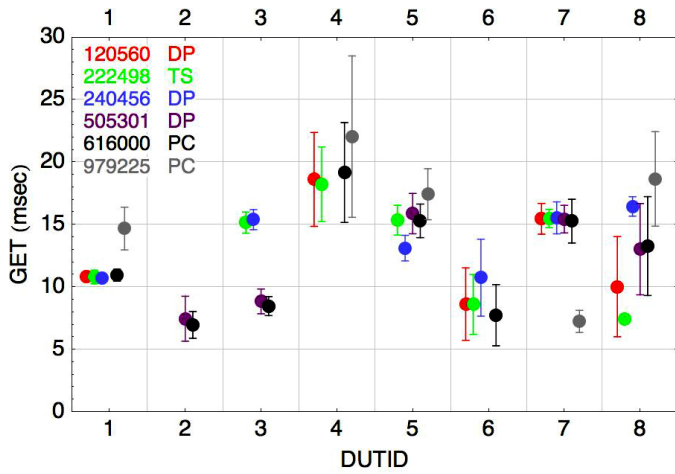


FIGURE 7 — Mean and standard deviation of GET estimates for eight DUT and six LMD.

both variation due to measurement error and due to genuine differences in BET with speed or gray level. These values are shown for all BET data in Fig. 6.

This figure shows that mean BET varies from about 7 to about 22 msec over the various displays. However, it also shows that there are significant differences among LMD when measuring the same DUT. These differences are evident both in the mean value, which may differ by as much as 90%, and also in the estimates of variation.

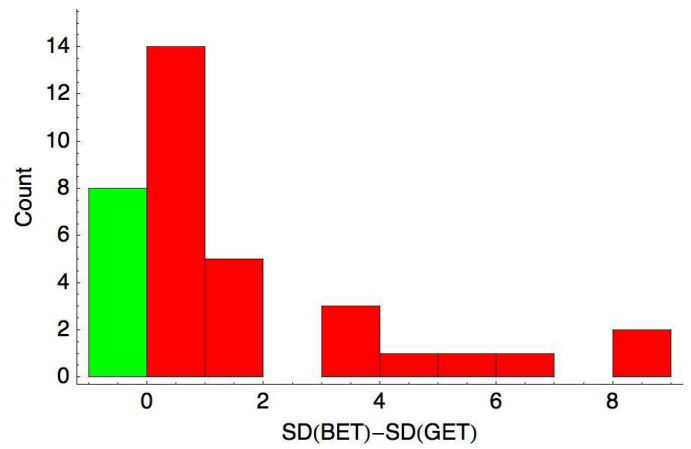


FIGURE 8 — Difference of standard deviations for GET and BET for corresponding LMD and DUT.

3.4 GET results

As noted above, it is possible to estimate BET directly from the Gaussian fit to the METP, using the metric GET. We have done this for all 1360 METP. In Fig. 7 we show these estimates. (This figure is almost identical to the figure produced for the subset of these estimates that correspond to the BET estimates in Fig. 3, except for the addition of LMDID 240456 at DUTID 006.) As expected, the values are generally similar to BET, but the variability of GET estimates is considerably lower.

The results at DUTID 003 require special comment. In this case two LMDs (240456 and 222498) measured the display driven at 60 Hz, while the other two (505301 and

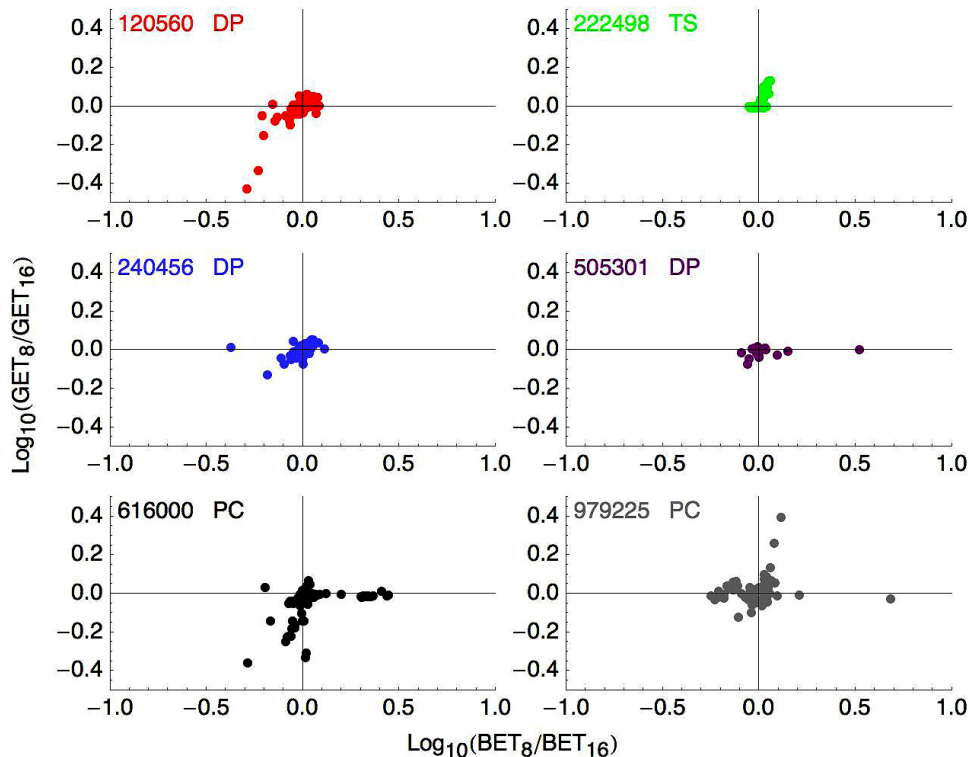


FIGURE 9 — Log of the ratio of BET estimates for 8 and 16 pixels/frame, compared to the corresponding quantity for GET.

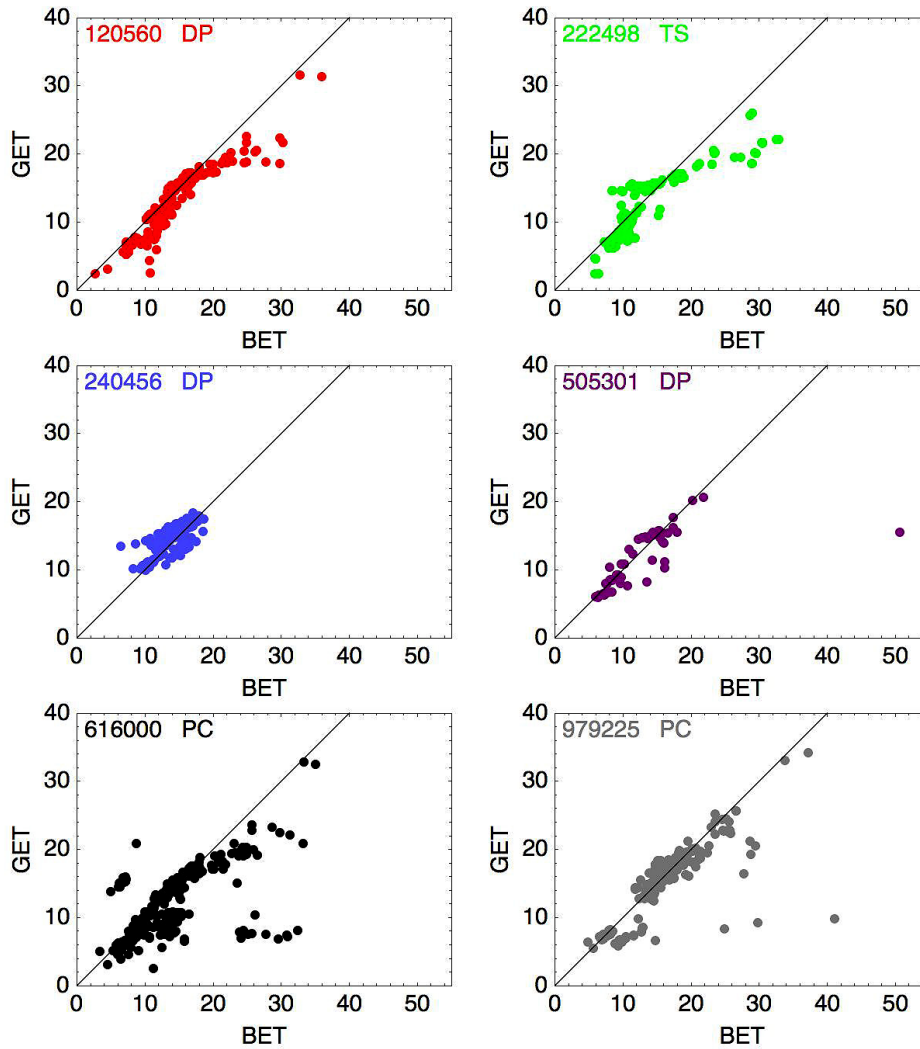


FIGURE 10 — Correlations of BET and GET. Each point is one condition (LMD, DUT, speed, gray levels). We omit one point at $\{\text{BET}, \text{GET}\} = \{78.5, 16.5\}$ for LMD 979225.

616000) used 120 Hz. Because GET (or BET) is largely proportional to hold time, we expect and find a difference of a factor of two between these values of GET.

Figures 6 shows that there are differences among BET estimates as provided by the various LMD, especially with respect to some of the displays (*e.g.*, DUT 003, 005, and 008). Figure 7 shows that some of this variation can be removed though use of a robust metric like GET. But Fig. 7 also shows that some discrepancies between LMD remain. These remaining discrepancies must be due to differences in the methods of acquiring (or reporting) the METP. This is analyzed in a later section.

The reduced variance of the GET metric, relative to BET, is shown more clearly in Fig. 8. This shows a histogram of differences between standard deviations for GET and BET for corresponding combinations of LMD and DUT. It shows that in a great majority of cases, GET yields a lower standard deviation and that in many cases the advantage is very large.

GET exhibits another advantage here as well. We were able to estimate values of GET from all 1360 METP records,

while only 1281 BET estimates were provided by the proponent teams. In short, 6% of BET estimates were missing. We speculate that the missing estimates are the result of the difficulty of estimating BET by locating 10% and 90% points in noisy waveforms with uncertain maxima and minima. This difficulty is obviated by the Gaussian fitting method of GET.

Under most conditions, estimates of BET or GET should be independent of speed. We looked at the log of the ratio between the two estimates for 8 and 16 pixels/frame. Departures from zero indicate a discrepancy between the two estimates. We then compared these log ratios for corresponding conditions for BET and GET, as shown in Fig. 9. The discrepancies are generally larger for BET. This illustrates another advantage of the GET metric over BET. However, both metrics exhibit discrepancies, which is a subject for concern and for further investigation. Note also that the discrepancies are not consistently either positive or negative, as might be expected of a systematic difference in display behavior between the two speeds. In comparing

LMDs, it must be noted that different LMDs measured different displays.

3.5 Correlation of BET and GET

Here, we compare the individual measurements of BET and GET for each condition (LMD, DUT, speed, and gray levels). This comparison is shown in Fig. 10 for all conditions for which we have BET estimates. The colors are the standard colors for each LMD, as used in Fig. 6. To save space, we omit one point at {BET, GET} = {78.5, 16.5}. A line is drawn to indicate identity between the two quantities. There is general agreement between the two estimates (Pearson correlation = 0.72). The points lie generally below the line, indicating that GET estimates are on average slightly smaller than BET. This is probably due to effects of overshoot or undershoot on BET. But it is also evident that for some cases, there are large departures from the line. We attribute these to poorly estimated values of BET that contribute to the increased variance of BET shown in Figs. 6–9. For example, compare the variance of LMDID 616000 shown in Figs. 6 and 7 and the black points in this figure.

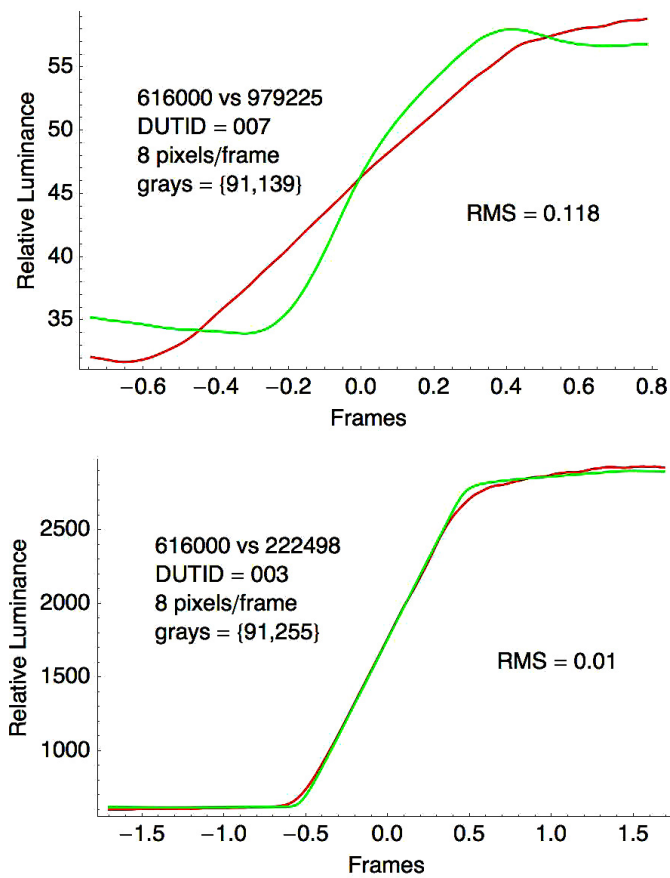


FIGURE 11 — Illustration of waveform difference metric. In each panel we show two smoothed waveforms derived from two different LMD for the same DUT, speed, and gray levels. The waveform difference (normalized RMS error) is shown. The lower panel shows a result near to the mode for all conditions tested (see Fig. 12).

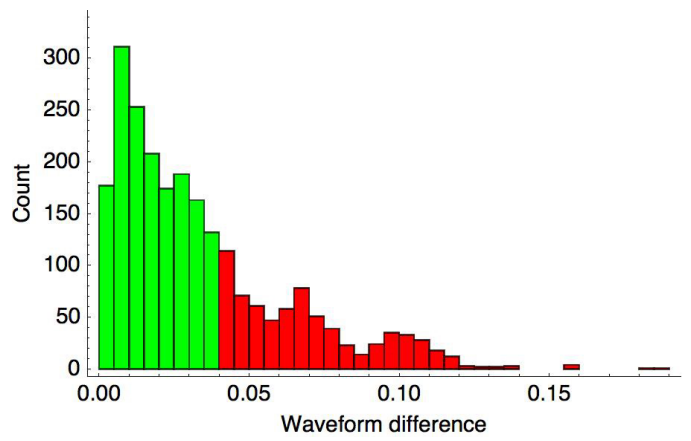


FIGURE 12 — Waveform difference between pairs of matching waveforms from different LMD but the same DUT, speed, and gray levels. Values greater than 0.04 are colored red.

3.6 Comparison of waveforms obtained by different LMD

Systematic comparisons between actual waveforms from different LMD are difficult because not all proponents collected data from the same DUT at the same gray levels and because different LMD do not generally use the same set of time samples. We have conducted the following analysis. For a pair of waveforms from the same DUT and two different LMD, we first conducted on each the Gaussian-fitting and smoothing operations as described in an earlier section. From this we obtained two smoothed waveforms, each centered at the mean of the fitted Gaussian, and trimmed to plus and minus four standard deviations (examples of smoothed trimmed waveforms are shown as the green curves in Fig. 2). We then performed a linear interpolation on each of the two resulting waveforms. We then found the

	222498	240456	505301	616000	979225
120560	0.99	1.9	1.6	1.1	5.6
222498		1.9	1.7	1.3	4.8
240456			2.4	2.	4.4
505301				0.75	4.2
616000					4.

FIGURE 13 — Median waveform difference for each pairing of LMDs. Values less than 0.02 are green, less than 0.04, yellow, and greater than 0.04, red. The printed median values are multiplied by 100 for clarity.

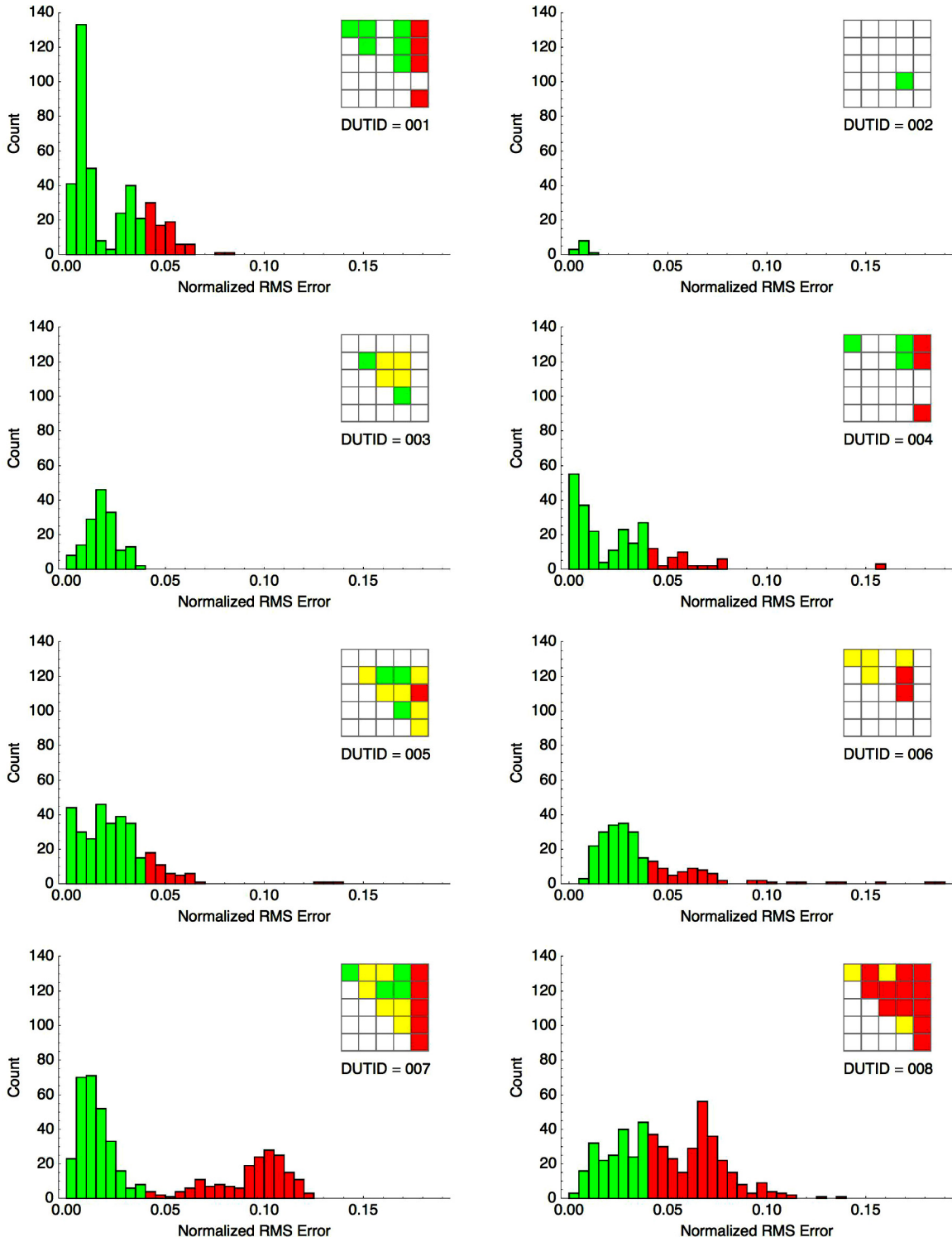


FIGURE 14 — Distributions of waveform difference between METP obtained from different LMD for the same DUT, speed, and gray levels. Each panel is for a different DUTID. The small inset matrices shown the pairwise medians, as in Fig. 13.

linearly transformed version of the second curve that was the closest match to the first curve, as determined by squared differences between 100 samples points of the interpolation. Finally, we computed the normalized RMS error between the two matched curves, which we will call the *waveform difference*. Two examples are shown in Fig. 11, one showing a case with a large difference between

the two transformed waveforms, and the other a small difference, near to the mode of the distribution of differences.

To analyze the total set of waveforms, we applied this metric to all pairs of METP that matched in DUT, speed, and gray levels, but differed in LMD. There were 2328 such cases. Note that LMDID 240456 used “symbolic” gray levels of integers 0 through 4. We approximated these with the

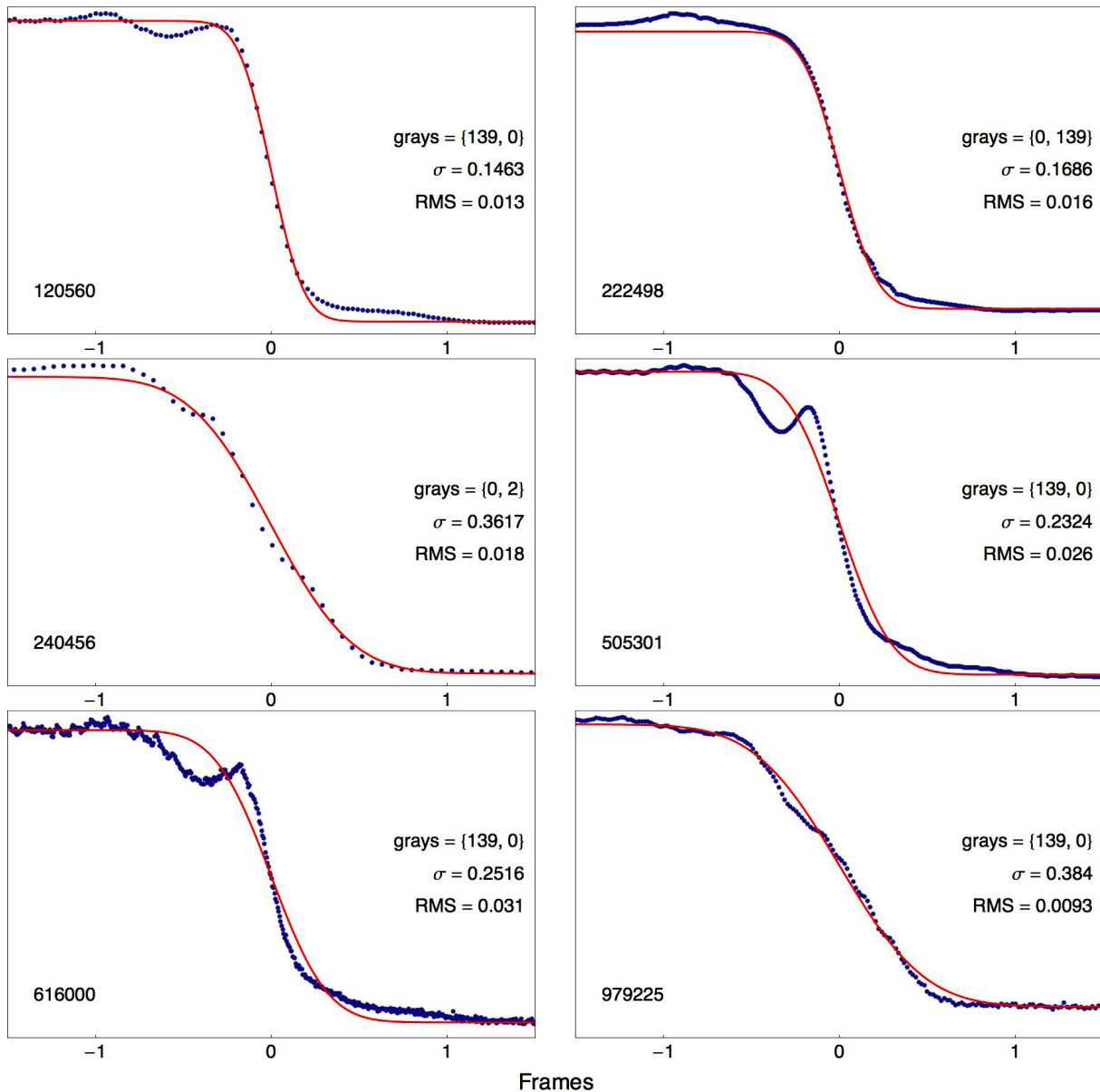


FIGURE 15 — METP waveforms for six different LMDs from the same conditions on DUT 008. The gray levels were {139,0} and the speed was 8 pixels/frame. The red curve is the fitted Gaussian and the value of σ is given in frames, along with the RMS error of the fit of the Gaussian.

standard levels of {0, 91, 139, 150, 255} for this analysis. In Fig. 12, we plot the distribution of metric values for all cases. We color red those cases greater than 0.04 (the 0.7 quantile).

To provide some insight into which LMD agree and which differ, the matrix in Fig. 13 shows the median waveform difference over all cases for each pair of LMDs, color coded as green (<0.02), yellow (<0.04, and red (>0.04). It is clear that most LMD generally agree, but that LMDID 979225 differs markedly from all the others.

Finally, we look at the waveform difference for individual DUT in Fig. 14. In each panel we also show a small version of the matrix as in Fig. 13 to show which LMD pairs are disagreeing. This figure confirms is that LMDID 979225 is discrepant, but also shows that certain DUTs (*e.g.*, 008) cause discrepancies for other LMD as well.

To illustrate further the differences among LMD, significant Fig. 15 shows the METP captured by the six different LMD for one speed and gray-level pair. Clearly, the waveforms are significantly different, as are the widths of the transition, as reflected in the indicated values of σ . We should note that this display, with a scanning backlight, was one of the most challenging.

4 Discussion

4.1 Individual LMD

Here, we provide some brief comments on individual LMD. When we refer to the consensus mean we exclude 979225, for reasons detailed below.

4.1.1 120560 (DP)

This LMD yielded mean GET estimates very near to the consensus mean for the five DUT tested, and except for DUT 008 (SBL) it had low variance (Fig. 7). Estimates of GET were generally slightly lower for GET than for BET, but otherwise very well correlated (Fig. 10). The waveforms acquired by this LMD generally agreed with other LMD, except for DUT 008, and LMD 979225 (Figs. 13 and 14). This LMD showed some large discrepancies between GET for the two speeds, for unknown reasons (see Fig. 9).

4.1.2 222498 (TS)

This LMD yielded mean GET estimates very close to the consensus mean for the six of the DUT tested, but somewhat lower at DUT 008 (Fig. 7). It had the lowest variance. GET and BET were well correlated. The waveforms acquired by this LMD generally agreed with other LMD, except for DUT 008, and LMD 979225 (Figs. 13 and 14).

4.1.3 240456 (DP)

This LMD yielded mean GET estimates close to the consensus mean for the three of the DUT tested, but departed somewhat at DUT 005, 006, and 008 (Fig. 7). It had low variance. GET and BET were well correlated. The waveforms acquired by this LMD generally agreed with other LMD, except for DUTs 006 and 008, and LMD 979225 (Figs. 13 and 14).

4.1.4 505301 (DP)

This LMD yielded mean GET estimates among the closest, of all LMD, to the consensus mean for the five DUT tested (Fig. 7). Variance was similar to other LMD. Correlation between GET and BET was particularly high (0.91) but only when one very anomalous value of BET is omitted (see rightmost point in Fig. 10). We have examined the waveform for this condition, and find no explanation for the value of BET reported, and suspect it is a reporting error.

4.1.5 616000 (PC)

This was the only LMD used with all eight DUT. It yielded mean GET estimates among the closest, of all LMD, to the consensus mean for the eight DUT tested (Fig. 7). Variance was similar to that of other LMD. Figure 10 shows that while many estimates of GET and BET agree, a sizable fraction of BET estimates are very different. This is also evident in the much larger variances for BET than for GET in Figs. 6 and 7. We speculate that this LMD collects accurate waveforms but is less reliable at estimating BET from the waveform. This is also suggested by the large discrepancies between BET for the two speeds as shown in Fig. 9.

4.1.6 979225 (PC)

This LMD produces mean GET estimates that are generally discrepant from the consensus mean (Fig. 7). The discrepancies are not in a consistent direction, and may be as large as a factor two. Variances are higher, sometimes much higher than average. The estimates of GET and BET are well correlated, apart from some outliers (Fig. 10), which suggests that the problem is with the waveform collection itself. This is confirmed by Fig. 14, which shows that the waveforms for this LMD are markedly different from those for all other LMD. Because its performance is so discrepant from the other LMDs, we exclude it for the discussions below of individual DUT.

4.2 Individual DUT

Here, we provide some brief comments on the measurements for the various individual DUT. For each DUT, we indicate in the heading any special display features (see Table 1). For reference, the reader should consult Figs. 4, 6, 7, and 13. All comments exclude LMDID 979225, which we believe to be erroneous.

4.2.1 001 (BLI)

This DUT, which employs black level insertion, yields very similar estimates of BET and GET from four LMD, which include types DP, PC, and TS. The waveforms are very well fit by a Gaussian.

4.2.2 002 (HCFL, SBL, 120 Hz)

Only two LMD (DP and PC) were used on this DUT. The two estimates of GET are very close, those of BET slightly less close. The waveform differences are small, and the Gaussian fits moderately well.

4.2.3 003 (120 Hz)

Four LMD were used (TS, PC, DP, DP). The estimates of BET differ somewhat, and show large individual variance, while GET estimates shown very low variance, and are in close agreement (apart from a factor of two that results from differing frame rates during measurement). Waveform error is moderate and the Gaussian is a very good fit.

4.2.4 004

Mean BET estimates from three LMD (PC, TS, DP) are very close, but show large individual variance. GET estimates are also nearly identical, and show much lower variance. This DUT, unlike the previous three, shows significant variation in GET with gray level, which manifests as vari-

ance. The estimates of this variance are also quite close for the three LMD. The waveforms from this DUT are well fit by the Gaussian, and the waveform difference between LMD is small.

4.2.5 005 (OD)

Although this DUT uses overdrive, there is very little evidence of overshoot in the waveforms, which are fit very well by the Gaussian. The BET estimates show large variance both within LMD and between LMD, while the GET estimates show low variance in both cases. Waveform difference is low to moderate.

4.2.6 006 (PDP, OD)

This plasma panel shows some overshoot, and some ringing (see below) but is otherwise well fit by the Gaussian. Both BET and GET estimates for three LMD are in close agreement; a GET for a fourth LMD (240456), where no BET was reported, is slightly farther off. The waveform differences are moderate to large, the latter due primarily to large amounts of ringing shown by 616000 (PC). 222498 (TS) shows no ringing, while 120560 and 249456 (DP) show intermediate amounts. This appears to be a case where TS and the pursuit methods show somewhat different waveforms, though that does not lead to different estimates of GET.

4.2.7 007

This DUT was measured by all six LMD. Waveforms were generally very well fit by the Gaussian. A small amount of overshoot was evident for certain gray levels (*e.g.*, {0,139}), and was more evident for some LMD (*e.g.*, 616000) than others. BET estimates are in close agreement, as are GET estimates. Waveform differences were small to moderate, presumably due to overshoot.

4.2.8 008 (HCFL, SBL)

This DUT was tested by all six LMD, and showed the largest waveform differences. Examining the waveforms, it is evident that some LMD yield waveforms that are smooth and Gaussian with some small perturbations (120560 DP, 222498 TS, 240456 DP), while others show large deviations (505301 DP, 616000 PC). This difference appears not to depend on method.

Both estimates of BET and of GET are quite scattered, differing by as much as a factor of 2. LMD 222498 (TS) yields the smallest values, while 240456 yields the largest. These differences in GET (or BET) do not seem to be correlated with the fit of the Gaussian and remain unexplained. Another DUT (002) uses HCFL and SBL, but does

not seem to show these discrepancies. However, only two LMD were used on that display.

This DUT showed relatively large dependence of GET (or BET) on gray level.

5 Summary

We compared six different instruments taking measurements of motion blur on eight different displays. We found significant discrepancies between instruments, and large variability within single instruments. Both types of variability can be greatly reduced through the use of the robust GET estimation method, in which a Gaussian is fit to the moving edge temporal profile.

One of the LMD (979225) was sufficiently different from all other LMD that we conclude it was not functioning properly. This LMD was excluded from most subsequent comparisons.

Although our data are sparse in this regard, the three methods examined (PC, DP, and TS) all perform about equally well, though the one clearly anomalous case (979225) was an instance of PC.

Excluding the anomalous case, and using the robust GET method, the remaining discrepancies between instruments occur primarily for one DUT (008), which employed a scanning backlight. Further research will be required to determine the cause of these discrepancies, and the best method for estimating motion blur under these conditions.

Overall, these results show good agreement among devices and methods, but also show the need for further improvement, standardization, and evaluation of motion-blur measurement methods.

Acknowledgments

I thank all the members of the ICDM who provided data or other support for this project, especially Ed Kelly (NIST), Joe Miseli (Sun Microsystems and Oracle), and Jongseo Lee (Samsung). This work was supported in part by NASA's Space Human Factors Engineering Project, WBS 466199 and by NASA/FAA Interagency Agreement DTFAWA-08-X-80023.

Appendix

For reference, we have created a document illustrating the METP, smoothed waveform, and fitted Gaussian for all 1360 cases we collected. Each figure also shows the estimated value of sigma, and the normalized RMS error of the Gaussian fit. This document is available at <http://vision.arc.nasa.gov/projects/motionblur/jsid-metp-figures.pdf>.

References

- 1 S. Tourancheau *et al.*, "Visual annoyance and user acceptance of LCD motion-blur," *SID Symposium Digest* **40**, 919-922 (2009).
- 2 M. E. Becker, "Motion-blur evaluation: A comparison of approaches," *J. Soc. Info. Display* **16**, 989-1000 (2008).

- 3 X.-F. Feng *et al.*, "Comparisons of motion-blur assessment strategies for newly emergent LCD and backlight driving technologies," *J. Soc. Info. Display* **16**, 981–988 (2008).
- 4 K. Oka and Y. Enami, "Moving picture response time (MPRT) measurement system," *SID Symposium Digest* **35**, 1266 (2004).
- 5 A. B. Watson, "The spatial standard observer: A human vision model for display inspection," *SID Symposium Digest* **37**, 1312–1315 (2006).
- 6 F. H. van Heesch *et al.*, "Characterizing displays by their temporal aperture: A theoretical framework," *J. Soc. Info. Display* **16**, 1009–1019 (2008).
- 7 H. Pan *et al.*, "LCD motion blur modeling and analysis," *Proc. IEEE Intl. Conf. on Image Processing* **2**, II-21–24 (2005).
- 8 X. Li *et al.*, "LCD motion artifact determination using simulation methods," *SID Symposium Digest* **37**, 6–9 (2006).
- 9 J. Miseli, "Introducing the International Committee for Display Metrology (ICDM)," *Information Display* **24** (2008).
- 10 S. Tourancheau *et al.*, "LCD motion-blur estimation using different measurement methods," *J. Soc. Info. Display* **17**, 239–249 (2009).
- 11 A. B. Watson, "Comparison of motion blur measurement methods," *SID Symposium Digest* **40**, 206–209 (2009).
- 12 S. Sluyterman, "Dynamic-scanning backlighting makes LCD TV come alive," *Information Display* **21**, 10–28 (2005).
- 13 T. Kurita, "Moving picture quality improvement for hold-type AM-LCDs," *SID Symposium Digest* **32**, 986–989 (2001).



Andrew B. Watson did undergraduate work at Columbia University and received his Ph.D. in psychology from the University of Pennsylvania in 1976. He subsequently held post-doctoral positions at the University of Cambridge in England and at Stanford University in California. Since 1980, he has worked at NASA Ames Research Center in California, where he is the Senior Scientist for Vision Research, and where he works on models of vision and their application to visual technology. He is the author of over 100 papers on topics such as spatial and temporal sensitivity, motion perception, image quality, and neural models of visual coding and processing. He is the author of five patents in areas such as image compression, video quality, and detection of artifacts in display manufacturing. In 2000, he founded the *Journal of Vision* (<http://journalofvision.org>) where he now serves as Editor-in-Chief. Dr. Watson is a Fellow of the Optical Society of America, a Fellow of the Association for Research in Vision and Ophthalmology, a Senior Member of the SID, and also serves as the Vice Chair for Vision Science and Human Factors of the International Committee on Display Measurement. In 1990, he received NASA's H. Julian Allen Award for outstanding scientific paper, and in 1993 he was appointed Ames Associate Fellow for exceptional scientific achievement. He is the 2007 recipient of the Otto Schade Award from the Society for Information Display, and the 2008 winner of the Special Recognition Award from the Association for Research in Vision and Ophthalmology.